

Lysophosphatidylcholine as an effector of fatty acid-induced insulin resistance[§]

Myoung Sook Han,^{1,*} Yu-Mi Lim,^{1,*} Wenyang Quan,^{*} Jung Ran Kim,[§] Kun Wook Chung,^{*} Mira Kang,[†] Sunshin Kim,^{**} Sun Young Park,^{*} Joong-Soo Han,^{††,§§} Shin-Young Park,^{††,§§} Hyae Gyeong Cheon,[§] Sang Dal Rhee,^{***} Tae-Sik Park,^{2,§} and Myung-Shik Lee^{2,*}

Department of Medicine* and Center for Health Promotion,[†] Samsung Medical Center, Sungkyunkwan University School of Medicine, Seoul 135-710, Korea; Lee Gil Ya Cancer and Diabetes Institute,[§] Gachon University School of Medicine and Science, Incheon 406-840, Korea; Carcinogenesis Branch,^{**} Korean National Cancer Center, Goyang 410-769, Korea; Institute of Biomedical Science^{††} and Department of Biochemistry and Molecular Biology,^{§§} College of Medicine, Hanyang University, Seoul 133-791, Korea; and Bio-Organic Science Division,^{***} Korea Research Institute of Chemical Technology, Daejeon 305-343, Korea

Abstract The mechanism of FFA-induced insulin resistance is not fully understood. We have searched for effector molecules(s) in FFA-induced insulin resistance. Palmitic acid (PA) but not oleic acid (OA) induced insulin resistance in L6 myotubes through C-Jun N-terminal kinase (JNK) and insulin receptor substrate 1 (IRS-1) Ser307 phosphorylation. Inhibitors of ceramide synthesis did not block insulin resistance by PA. However, inhibition of the conversion of PA to lysophosphatidylcholine (LPC) by calcium-independent phospholipase A₂ (iPLA₂) inhibitors, such as bromoenol lactone (BEL) or palmitoyl trifluoromethyl ketone (PACOCF₃), prevented insulin resistance by PA. iPLA₂ inhibitors or iPLA₂ small interfering RNA (siRNA) attenuated JNK or IRS-1 Ser307 phosphorylation by PA. PA treatment increased LPC content, which was reversed by iPLA₂ inhibitors or iPLA₂ siRNA. The intracellular DAG level was increased by iPLA₂ inhibitors, despite ameliorated insulin resistance. Pertussis toxin (PTX), which inhibits LPC action through the G-protein coupled receptor (GPCR)/G α_i , reversed insulin resistance by PA. BEL administration ameliorated insulin resistance and diabetes in *db/db* mice. JNK and IRS-1 Ser307 phosphorylation in the liver and muscle of *db/db* mice was attenuated by BEL. LPC content was increased in the liver and muscle of *db/db* mice, which was suppressed by BEL. **These findings implicate LPC as an important lipid intermediate that links saturated fatty acids to insulin resistance.**—Han, M. S., Y-M. Lim, W. Quan, J. R. Kim, K. W. Chung, M. Kang, S. Kim, S. Y. Park, J-S. Han, S-Y. Park, H. G. Cheon, S. D. Rhee, T-S. Park, and M-S. Lee. **Lysophosphatidylcholine as an effector of fatty acid-induced insulin resistance.** *J. Lipid Res.* 2011. 52: 1234–1246.

This study was supported by the 21C Frontier Functional Proteomics Project Grant FPR08B1-210 from the Korean Ministry of Science & Technology and the Korea Healthcare Technology R&D Project Grant A080967 from the Korean Ministry for Health, Welfare & Family Affairs. M-S. Lee is the recipient of the Bio R&D Program Grant 2008-04090 and Global Research Laboratory Grant K21004000003-10A0500-00310 from the National Research Foundation of Korea.

Manuscript received 4 March 2011.

Published, JLR Papers in Press, March 28, 2011
DOI 10.1194/jlr.M014787

Supplementary key words muscle • lipids • obesity • diabetes • phospholipase A₂

The two major elements in the pathogenesis of type 2 diabetes are insulin resistance and β -cell failure. The biochemical mechanisms underlying these two phenomena are incompletely understood. The plasma FFA level is commonly elevated in type 2 diabetes patients (1). Furthermore, previous studies have presented evidence suggesting that FFA released from visceral fat is one of the primary culprits in the pathogenesis of insulin resistance, which is a prerequisite for the development of type 2 diabetes (2). In addition to insulin resistance, relative insulin deficiency is necessary for the development of type 2 diabetes. In this step of β -cell failure, FFA has also been reported to play an important role as a potential effector of pancreatic β -cell dysfunction or death (lipotoxicity) (3, 4). Thus, chronically elevated FFA may contribute to both essential steps in the development of type 2 diabetes, and it represents one of the fundamental etiological mechanisms

Abbreviations: BEL, bromoenol lactone; DAG, diacylglycerol; GPCR, G-protein coupled receptor; HOMA-IR, homeostasis model assessment of insulin resistance; IPGTT, intraperitoneal glucose tolerance test; iPLA₂, calcium-independent phospholipase A₂; IRS-1, insulin receptor substrate 1; IIT, insulin tolerance test; JNK, C-Jun N-terminal kinase; LPC, lysophosphatidylcholine; OA, oleic acid; PA, palmitic acid; PACOCF₃, palmitoyl trifluoromethyl ketone; PAP, phosphatidic acid phosphatase; PC, phosphatidylcholine; PKC, protein kinase C; PTX, pertussis toxin; siRNA, small interfering RNA; SPT, serine palmitoyl transferase; TG, triglyceride.

¹M-S. Han and Y-M. Lim contributed equally to this work.

²To whom correspondence should be addressed.

e-mail: mslee0923@skku.edu (M-S.L.); tspark@gachon.ac.kr (T-S.P.)

[§]The online version of this article (available at <http://www.jlr.org>) contains supplementary data in the form of five figures.

underlying the complicated and diverse manifestations of type 2 diabetes, obesity, and metabolic syndrome.

Despite strong epidemiological and *in vivo* data suggesting a relationship between FFA and type 2 diabetes, a detailed molecular and cellular mechanism underlying insulin resistance has not been clearly elucidated. Recent studies have dissected the metabolic pathway to unravel the intracellular mechanism of insulin resistance by FFA. The results of such studies have implicated diacylglycerol (DAG), ceramide, triglyceride (TG), or other metabolites arising from incomplete β -oxidation of fatty acids as the final effector molecules inducing insulin resistance or lipotoxicity (5–8). However, it remains controversial which metabolites produced from FFA are directly responsible for the insulin resistance or β -cell failure by FFA.

We have studied the mechanism of lipoapoptosis using various pharmacological inhibitors (9). In this investigation, we employed the same pharmacological strategy to determine the mechanism of insulin resistance by FFA, and we found evidence favoring the role of LPC produced from FFA in insulin resistance *in vitro* and *in vivo*.

MATERIALS AND METHODS

Cell culture

L6 myoblasts (kindly provided by Dr. Lee Wan, College of Medicine, Dongguk University, Kyungju, Korea) were grown in α -MEM (Gibco-BRL, Grand Island, NY)-10% FBS. For differentiation, 4×10^4 /ml L6 myoblasts were plated in 60 mm dishes and cultured in α -MEM 10% FBS for 24 h. The medium was replaced with α -MEM 2% FBS to induce fusion of myoblasts to myotubes (10). Formation of myotubes was monitored by phase contrast microscopy. Differentiation medium was replenished every 24–48 h. Mature myotubes formed within 6–8 days after seeding.

Reagents

BEL was purchased from Cayman (Ann Arbor, MI). Fumonisin B1 and palmitoyl trifluoromethyl ketone (PACOCF₃) were from Calbiochem (San Diego, CA). All other chemicals were obtained from Sigma (St. Louis, MO) unless stated otherwise.

FFA treatment

The palmitic acid (PA) solution was made according to a previously published protocol with modifications (11). Briefly, a PA stock solution (50 mM) was prepared by dissolving PA in 70% ethanol and heating at 50°C. The working PA solution was made by diluting stock solution in α -MEM 2% FFA-free BSA 2% FBS, then filtered before use.

Measurement of LPC

The intracellular LPC content was measured using an enzymatic assay as previously reported (9). Briefly, the sample was added to a mixture of 100 mM Tris-HCl (pH 8.0), 0.01% Triton X-100, 1 mM CaCl₂, 3 mM *N*-ethyl-*N*-[2-hydroxy-3-sulfo-propyl]3-methylaniline, 10 U/ml peroxidase, 0.1 U/ml glycerophosphorylcholine phosphodiesterase, and 10 U/ml choline oxidase. After incubation at 37°C for 5 min, the reagent mixture containing 100 mM Tris-HCl (pH 8.0), 5 mM 4-aminoantipyrine, 0.01% Triton X-100, and 20 U/ml lysophospholipase was added. After incubation for another 5 min, A₅₇₀ was measured using LPC 16:0 as a standard.

Effect of iPLA₂ siRNA

L6 myotubes were transfected with calcium-independent phospholipase A2 (iPLA₂) β small interfering RNA (siRNA) (forward, AAC UCC UCA UUA UUC UCU GUG CUG CCU GUC UC; reverse, AAC AGC ACA GAG AAU GAG GAG CCU GUC UC), iPLA₂ γ siRNA (forward, AAG UAU UGC UAA CUU CCU UUC TT; reverse, GAA AGG AAG UUA GCA AUA CUU TT), or an irrelevant control siRNA as described (9). Expression of iPLA₂ β or iPLA₂ γ in siRNA-transfected myotubes was examined by RT-PCR using specific primer sets (iPLA₂ β forward, GTG ACA GTG AGA TCC TGG TG; reverse, CTT CAT GGC TGT GTG GAT GG; iPLA₂ γ forward, TAC ATT GGT GGA CTT GTA CCC; reverse, CAT CCT TAA CTT GTC TCA GCC).

DAG measurement

DAG was extracted from the cell pellet with chloroform/methanol (2:1, v/v) containing 0.01% butylated hydroxytoluene. A known amount of 1,2-dipentadecanoin was added as an internal standard. After vortexing and centrifugation, the lower phase was collected. Samples were evaporated and dissolved in hexane/methylene chloride/methyl *tert*-butyl ether for loading onto a diol-bonded solid phase extraction column (Waters, Inc., Milford, MA) under vacuum. DAG was eluted as described previously (12). The extracted lipids were dried under N₂ and redissolved in methanol. Then, the DAG content among extracted lipids was measured by LC-MS/MS using a bench-top tandem mass spectrometer (API 4000 Q-trap; Applied Biosystems, Framingham, MA) interfaced with an atmospheric pressure chemical ionization source and Agilent series 1200 micro-pump equipped with an autosampler as described (13). Five selected DAG species (di-16:0, di-18:1, 16:0-18:1, 18:0-18:2, and 18:0-20:4) were separated by HPLC with a phenyl column and ionized in the positive atmospheric pressure chemical ionization mode. [M+H-18]/product ions from corresponding DAG were monitored for multiple reaction monitoring quantitation of DAG. The mobile phase was 98% methanol with a flow rate of 0.25 ml/min, and 10 μ l sample was injected.

Ceramide measurement

The ceramide content was measured by LC-MS/MS using a previously reported method (14) with modifications. After lysis of cells in PBS, a known amount of C17:0-ceramide was added to the cell extracts as an internal standard. The phospholipids were extracted using chloroform/methanol, and then saponified by adding KOH and incubating at 37°C for 2 h. Extracts were centrifuged, and supernatants were isolated and dried under N₂. Ceramides (C14:0, C16:0, C18:0, C18:1, C20:0, C24:0, and C24:1), sphinganine, sphingosine, sphingosine-1-phosphate, and sphingomyelins (C16:0, C18:0, and C18:1) were separated by HPLC with C18 columns (XTerra C18, 3.5 μ m, 2.1 \times 50 mm) and ionized in the positive electrospray ionization mode. Metabolites of sphingolipids and ceramides were monitored for multiple reaction monitoring quantification by a bench-top tandem mass spectrometer (API 4000 Q-trap) interfaced with an electrospray ionization source.

TG measurement

TG was measured as previously described (9). In short, cells were fixed with 10% formaldehyde for 1 h. After staining with 3 μ g/ml Oil Red O solution for 15 min, dye was extracted by isopropanol and A₅₄₀ measured.

Western blotting

Western blotting was performed as described (15) using anti-phospho-C-Jun N-terminal kinase (JNK) Thr183/Tyr185, anti-insulin receptor substrate 1 (IRS-1), anti-Akt, anti-phospho-Akt

Ser473, Thr308 (Cell Signaling, Beverly, MA), anti-phospho-IRS-1 Ser307 (Upstate Biotechnology, Lake Placid, NY), anti-phospho-IRS-1 Tyr612 (Biosource International, Camarillo, CA), and anti-JNK antibodies (Santa Cruz Biotechnology, Inc., Santa Cruz, CA).

Glucose uptake

Uptake of 2-deoxyglucose was determined as previously described (16). Briefly, after starvation of L6 myotubes in serum-free α -MEM for 2 h, cells were incubated in α -MEM containing 100 nM insulin at 37°C for 30 min. After washing in HEPES buffer [20 mM Na-HEPES (pH 7.4) 140 mM NaCl, 5 mM KCl, 2.5 mM MgSO₄, and 1 mM CaCl₂], the cells were incubated in HEPES buffer containing 10 μ M 2-deoxyglucose and 0.5 μ Ci/ml 2-deoxy-D-[³H]glucose (Amersham, Piscataway, NJ) for 10 min. The reaction was stopped by washing with ice-cold 0.9% NaCl. The cells were solubilized in 1.5 ml 0.05 N NaOH for 30 min to measure [³H]glucose uptake using a scintillation counter. Nonspecific glucose uptake was measured in the presence of 10 μ M cytochalasin B and subtracted from the total uptake to calculate the specific uptake.

In vivo effect of iPLA₂ inhibitors

BEL was dissolved in a solution of 5% ethanol, 40% polyethylene glycerol 400, 15% cremophor EL, and 40% PBS, and then 200 μ g/kg of BEL was injected intraperitoneally to C57BL/Ks *db/db* mice three times a week for four weeks beginning at five weeks of age. Control *db/db* mice were injected with vehicle only. An intraperitoneal glucose tolerance test (IPGTT) was carried out after overnight fasting by an intraperitoneal injection of 1 gm/kg of glucose (17). Blood glucose concentrations were determined with an Accu-Chek glucometer (Roche, Mannheim, Germany) before (0 min) and 15, 30, 60, and 120 min after the injection of glucose. The homeostasis model assessment of insulin resistance (HOMA-IR) index was calculated as described (18). Serum insulin concentrations were determined using a commercial RIA kit for rat/mouse insulin measurement (Linco, St. Charles, MO). An insulin tolerance test (ITT) was conducted by intraperitoneal injection of 1 U/kg regular insulin to fasted mice as previously described (15). To study insulin signaling in vivo, 5 U/kg regular insulin (Novo Nordisk, Bagsvaerd, Denmark) was injected into the tail vein. At 5 Five min after insulin infusion, the liver and muscle tissue were removed and frozen in liquid nitrogen until use. All animal experiments were conducted in accordance with the Public Health Service Policy in Humane Care and Use of Laboratory Animals, and were approved by the Institutional Review Board of Samsung Medical Center Animal Facility.

β -cell mass

The pancreatic β -cell mass was measured by point counting morphometry after insulin immunohistochemistry of pancreatic sections was carried out as previously described (15).

Statistical analysis

All values are expressed as the means \pm SE from two to four independent experiments performed in triplicate to ensure reproducibility. Two-tailed Student's *t*-test was employed to compare the values between two groups. *P* values less than 0.05 were considered to represent statistically significant differences.

RESULTS

Insulin resistance by FFA

We first studied the effect of PA, the most abundant saturated FFA, on insulin signaling in differentiated L6

myotubes. Insulin induced phosphorylation of Akt Ser473 and IRS-1 Tyr612, indicating that insulin signaling was intact in differentiated L6 myotubes. Pretreatment with 600–1,000 μ M PA for 12 h induced significant attenuation of Akt Ser473 and IRS-1 Tyr612 phosphorylation in response to insulin, suggesting that PA inhibits insulin signaling (Fig. 1A). PA treatment also significantly decreased the insulin-induced uptake of 2-deoxyglucose, indicating that PA induces insulin resistance ($P < 0.05$) (Fig. 1B). In contrast, oleic acid (OA), the most abundant unsaturated FFA in vivo, did not significantly affect insulin-induced phosphorylation of Akt Ser473 or IRS-1 Tyr612 (Fig. 1A). In addition, OA did not affect glucose uptake after insulin treatment in L6 myotubes, suggesting a difference between saturated versus unsaturated FFA ($P > 0.05$) (Fig. 1B).

We next studied the signal transduction related to the PA-induced insulin resistance. We investigated whether PA affects JNK phosphorylation, which is critically involved in obesity-induced insulin resistance (19, 20). Treatment with 800 μ M PA for 6–12 h induced a substantial JNK phosphorylation in L6 myotubes as evidenced by increased phospho-p54 and phospho-p46 JNK bands, suggesting a role for JNK activation in PA-induced insulin resistance (Fig. 1C). We also examined whether PA induces Ser307 phosphorylation of IRS-1 since previous studies have shown that IRS-1 Ser307 phosphorylation by activated JNK attenuates tyrosine phosphorylation of IRS-1 by insulin (19, 21). Indeed, treatment with 800 μ M PA induced a significant phosphorylation of IRS-1 Ser307 (Fig. 1C). Furthermore, SP600125, a JNK inhibitor, remarkably attenuated IRS-1 Ser307 phosphorylation by PA (Fig. 1D), suggesting that JNK phosphorylation by PA leads to IRS-1 Ser307 phosphorylation and insulin resistance. The effect of PA on the phosphorylation of JNK and IRS-1 Ser307 was observed in a dose-dependent manner between 100 and 800 μ M (supplementary Fig. 1).

In contrast to PA, OA did not induce JNK or IRS-1 Ser307 phosphorylation (Fig. 1E), consistent with the absence of effects on the insulin-induced glucose uptake or Akt phosphorylation (Fig. 1A, B). Notably, OA induced a weak JNK activation 15 min after treatment, which might be through a mechanism distinct from PA-induced JNK activation (Fig. 1E).

LPC as a mediator of PA-induced insulin resistance

Because PA is converted to diverse lipid intermediates, such as ceramides, intracellularly and ceramides have been reported to activate protein kinase C (PKC) and inhibit insulin signaling (4, 5), we asked whether intracellular conversion of PA to ceramide is responsible for the insulin resistance induced by PA. We first studied the effect of Fumonisin B1, which blocks ceramide synthesis by inhibiting sphingosine *N*-acyltransferase (ceramide synthase) (22, 23), on insulin signaling and glucose uptake. Fumonisin B1 did not reverse impaired insulin-induced Akt Ser473 or IRS-1 Tyr612 phosphorylation by PA in L6 myotubes (Fig. 2A). Fumonisin B1 also did not affect reduced insulin-induced 2-deoxyglucose uptake by PA

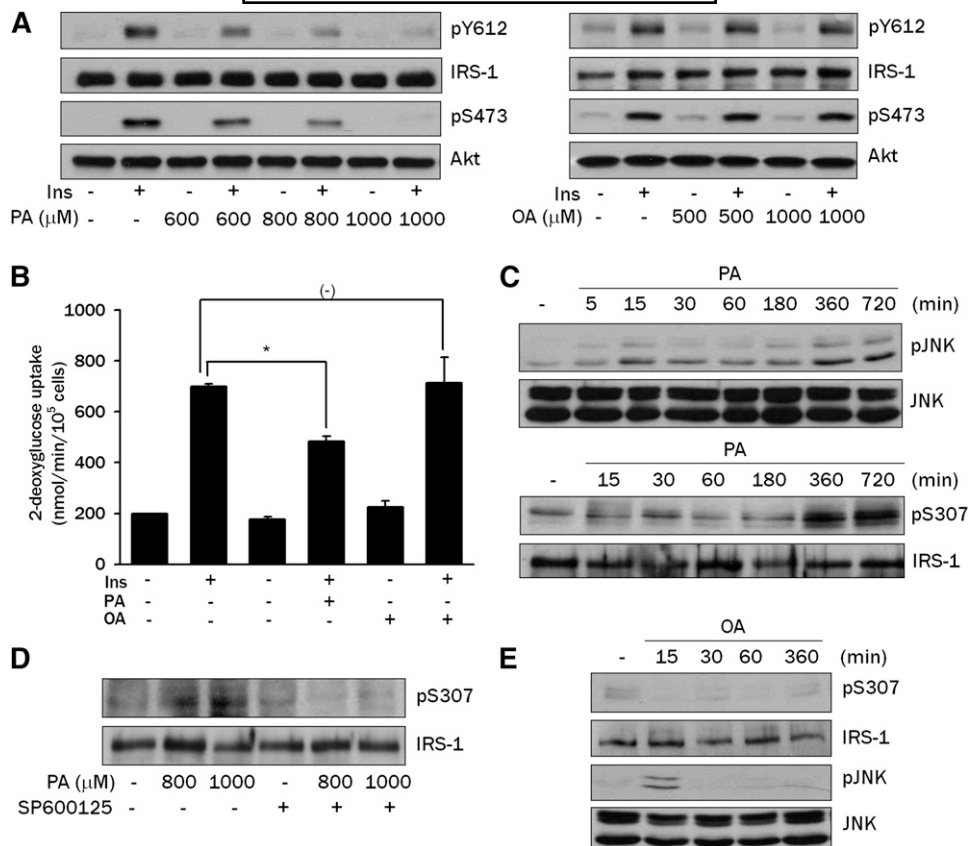


Fig. 1. Effects of PA on insulin signaling in L6 myotubes. **A:** L6 myotubes were incubated with the indicated concentrations of PA or OA for 12 h, then treated with 100 nM insulin for 15 min. Phosphorylation of IRS-1 Tyr612 and Akt Ser473 were evaluated by Western blot analysis using specific antibodies. **B:** L6 myotubes were incubated with 800 μ M PA or 1,000 μ M OA for 12 h. During the last 30 min of the incubation, cells were treated with 100 nM insulin, then uptake of 2-deoxyglucose was measured as described in Materials and Methods. **C:** L6 myotubes were treated with 800 μ M PA for the indicated time periods. Phosphorylation of JNK and IRS-1 Ser307 were examined by Western blot analysis using specific antibodies. **D:** L6 myotubes were treated with PA for 12 h in the presence of 20 μ M SP600125, a JNK inhibitor, and phosphorylation of IRS-1 Ser307 was evaluated as in C. **E:** L6 myotubes were treated with 500 μ M OA for the indicated time periods. Phosphorylation of JNK and IRS-1 Ser307 was evaluated as in C. The values in B (means \pm SE) are representative of three independent experiments performed in triplicate showing similar tendencies. Western blots are representative of three independent experiments showing similar features. * $P < 0.05$.

($P > 0.05$) (Fig. 2B). Because these results are in contrast to previous studies reporting an important role of de novo ceramide synthesis in insulin resistance, we next used Myriocin, which inhibits the first step of de novo ceramide synthesis by specifically inhibiting serine palmitoyltransferase (SPT) (24, 25). Myriocin did not reverse impaired insulin-induced Akt Ser473 or IRS-1 Tyr612 phosphorylation by PA in L6 myotubes (Fig. 2A), suggesting that conversion of PA to ceramide is not responsible for insulin resistance induced by PA. Myriocin also did not reverse the reduced insulin-induced glucose uptake by PA ($P > 0.05$) (Fig. 2B). Further, Fumonisin and Myriocin did not prevent PA-induced JNK activation (Fig. 2C). LC-MS/MS showed that the total ceramide content, which was markedly increased after PA treatment ($P < 0.005$), was significantly reduced by pretreatment with Fumonisin B1 or Myriocin ($P < 0.005$ for both comparisons) (Fig. 2D), indicating that ceramide synthesis was suppressed by chemical inhibitors as expected but that insulin resistance was not ameliorated despite successful suppression of ceramide content.

Next, we studied which intracellular lipid intermediates other than ceramide are involved in PA-induced insulin resistance. We have reported that DAG generated from PA could be further converted to phosphatidylcholine (PC), then to LPC, a well-known activator of JNK (26), by iPLA₂ (9). Because LPC is able to induce insulin resistance when administered exogenously (27), we investigated whether conversion of PA to LPC plays a role in the PA-induced JNK activation and insulin resistance. When L6 myotubes were pretreated with PACOCF₃ or BEL that could inhibit conversion of PA to LPC by inhibiting iPLA₂ (9), JNK phosphorylation by PA was substantially decreased, suggesting that endogenous LPC produced from PA induces JNK activation (Fig. 3A). IRS-1 Ser307 phosphorylation by PA was also reduced by PACOCF₃, which is consistent with the decreased JNK phosphorylation by PACOCF₃ or BEL (Fig. 3A). Additionally, PACOCF₃ or BEL reversed the decreased insulin-induced Akt Ser473 and IRS-1 Tyr612 phosphorylation by 800 μ M PA (Fig. 3B). Consistent with the decreased JNK phosphorylation and increased insulin-

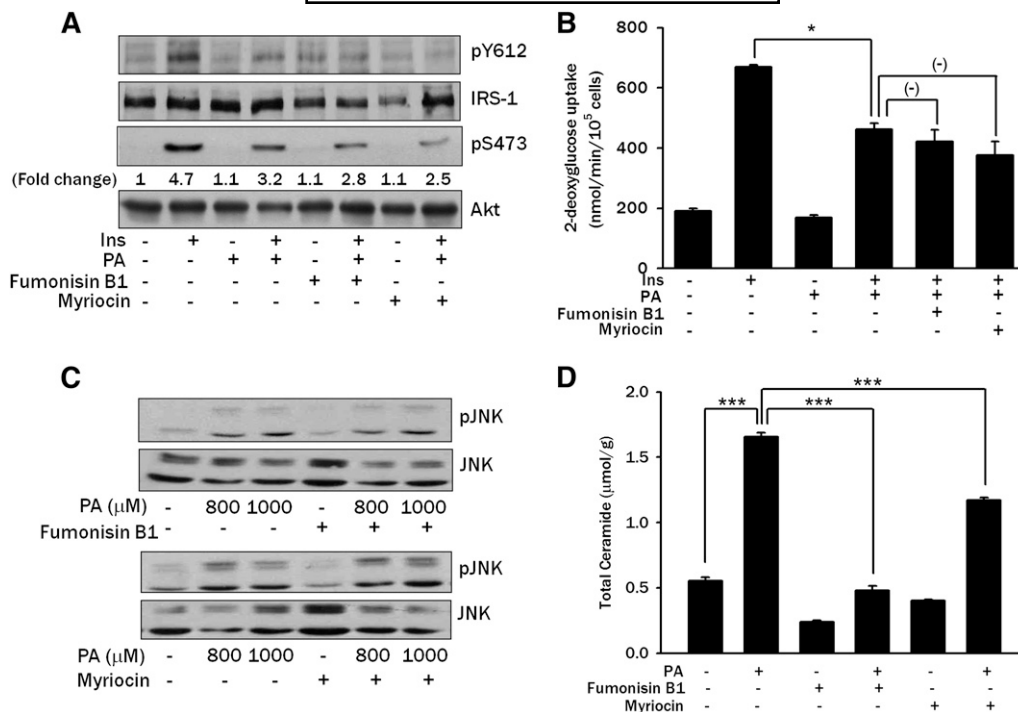


Fig. 2. Effect of ceramide synthesis inhibitors on PA-induced insulin resistance. **A:** L6 myotubes were pretreated with 20 μM Fumonisin B1 or 500 nM Myriocin for 1 h, then incubated with 800 μM PA for 14 h. Subsequently, L6 myotubes were treated with 100 nM insulin for 15 min, followed by Western blot analysis to determine phosphorylation of IRS-1 Tyr612 and Akt Ser473 using specific antibodies. Fold changes of the intensities of phospho-Akt Ser473 bands assessed by densitometry are shown. **B:** L6 myotubes were treated with 800 μM PA for 14 h after pretreatment with 20 μM Fumonisin B1 or 500 nM Myriocin for 1 h. During the last 30 min, myotubes were treated with 100 nM insulin, and uptake of 2-deoxyglucose was measured as in Fig. 1B. **C:** L6 myotubes were pretreated with 20 μM Fumonisin B1 or 500 nM Myriocin for 1 h, then incubated with PA for 12 h. Western blotting was done to evaluate JNK phosphorylation using a specific antibody. **D:** L6 myotubes were pretreated with Fumonisin B1 or Myriocin, then incubated with PA as in C. After lipid extraction, ceramide content was measured by LC-MS/MS as described in Materials and Methods. The values (means ± SE) are representative of two or three independent experiments performed in triplicate showing similar tendencies. Western blots are representative of four independent experiments showing similar features. * $P < 0.05$; *** $P < 0.005$.

induced Akt phosphorylation, PACOCF₃ reversed the reduced insulin-induced 2-deoxyglucose uptake by PA ($P < 0.05$) (Fig. 3C). Because the pharmacologic inhibitors we used could have off-target effects, we next employed genetic approaches. Transfection of iPLA₂β or iPLA₂γ siRNA or their combination decreased JNK phosphorylation by PA, suggesting potential involvement of multiple types of iPLA₂ in the conversion of PA to LPC in L6 myotubes (Fig. 3D).

Because these results suggested a role for LPC in PA-induced insulin resistance, we examined whether LPC content is increased by PA treatment of L6 myotubes. Indeed, treatment of L6 myotubes with 600–1,000 μM PA significantly increased LPC content ($P < 0.01$ – 0.05), while OA did not affect intracellular LPC content ($P > 0.05$) (Fig. 4A), which supports the idea that LPC is one of the important lipid metabolites of PA leading to insulin resistance. Treatment with PACOCF₃ or BEL, which ameliorated JNK activation by PA (Fig. 3A), markedly attenuated the increase in LPC content by PA ($P < 0.05$ and $P < 0.05$, respectively) (Fig. 4B), supporting the finding that LPC converted from PA induces JNK activation and insulin

resistance in L6 myotubes. Transfection of iPLA₂β or iPLA₂γ siRNA, which attenuated JNK activation by PA (Fig. 3D), also significantly suppressed the increase of LPC content after PA treatment ($P < 0.005$) (Fig. 4C).

We also measured DAG that could be produced intracellularly from PA and has been implicated as an effector molecule in FFA-induced insulin resistance (7). Total intracellular DAG content in L6 myotubes was significantly increased by treatment with 600 μM PA ($P < 0.005$) (Fig. 4D). The addition of PACOCF₃ further increased the total DAG content in L6 myotubes ($P < 0.005$) (Fig. 4D) despite improved insulin sensitivity (Fig. 3A–C). These results are attributable to the inhibition of iPLA₂ by PACOCF₃ at the distal step of DAG synthesis and suggest that amelioration of insulin resistance by PACOCF₃ is probably not related to DAG. The addition of BEL also increased the total intracellular DAG level in L6 myotubes; however, the increase was not significant ($P > 0.05$) (Fig. 4D), probably because BEL inhibits phosphatidic acid phosphatase (PAP) in addition to iPLA₂ (28). When individual molecular DAG species were analyzed, the contents of di-16:0 and 16:0-18:1 were most conspicuously increased after PA treatment and

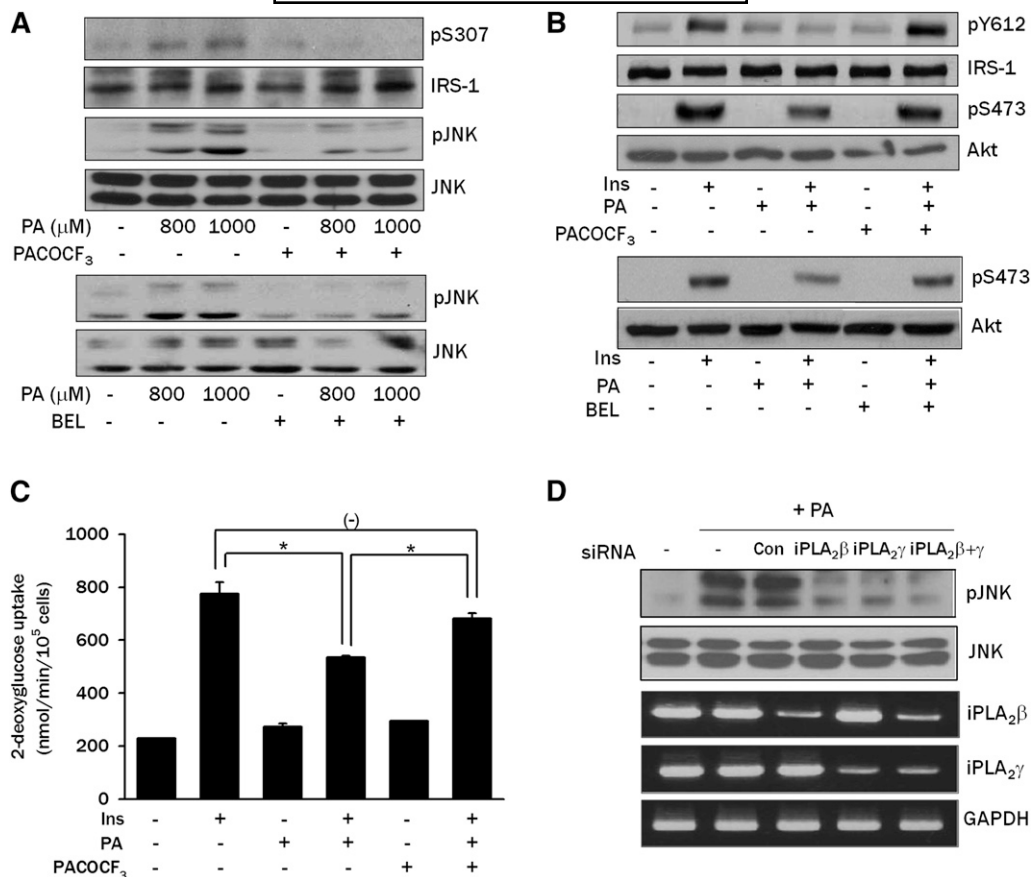


Fig. 3. Effect of iPLA₂ inhibitors or iPLA₂ siRNA on PA-induced insulin resistance. **A:** L6 myotubes were pretreated with 100 μM PACOCF₃ or 10 μM BEL, inhibitors of iPLA₂, for 1 h, then incubated with PA for 12 h. Phosphorylation of IRS-1 Ser307 and JNK was determined as in Fig. 1C. **B:** L6 myotubes were pretreated with PACOCF₃ or BEL, then with PA as in A. During the last 15 min, cells were treated with 100 nM insulin, and phosphorylation of IRS-1 Tyr612 and Akt Ser473 was determined as in Fig. 1A. **C:** L6 myotubes were pretreated with PACOCF₃, then with PA as in A. During the last 30 min, cells were treated with 100 nM insulin, and uptake of 2-deoxyglucose was measured as in Fig. 1B. **D:** L6 myotubes were transfected with iPLA₂β siRNA, iPLA₂γ siRNA or an irrelevant control siRNA (Con). After treatment with 800 μM PA for 12 h, JNK phosphorylation was determined as in Fig. 1C. Expression of iPLA₂β and iPLA₂γ was examined by RT-PCR using specific primer sets. The values in C (means ± SE) are representative of three independent experiments performed in triplicate showing a similar tendencies. Western blots and RT-PCR are representative of three or four independent experiments showing similar features. **P* < 0.05.

further enhanced by combined treatment with PACOCF₃ (supplementary Fig. II). These results are consistent with a previous study showing predominant production of di-16:0 phosphatidic acid after PA treatment (29) and again suggest attenuation of insulin resistance independent of DAG content. Changes in other DAG species were much less significant or insignificant compared with those of di-16:0 and 16:0-18:1 DAG (data not shown). Because changes in lipid droplet size due to increased TG content might lead to the sequestration of DAG or other bioactive lipid metabolites and dissociation of total DAG content versus bioactive DAG involved in lipid signaling, we measured TG content after treatment of L6 myotubes with FFA. TG content was not significantly affected by treatment with 600 μM PA that increased DAG concentration (Fig. 4D and supplementary Fig. III), eliminating the possible interference in DAG measurement. In contrast, TG content was significantly increased by 500 μM OA, showing difference between saturated versus unsaturated FFA (supplementary Fig. III).

Because PA could be converted to LPC in L6 myotubes, we studied whether LPC impairs insulin signaling directly. Exogenous LPC attenuated the phosphorylation of IRS-1 Tyr612 and Akt Ser473 in response to insulin (Fig. 5A). LPC also induced IRS-1 Ser307 and JNK phosphorylation (Fig. 5B), indicating that exogenous LPC inhibits insulin signaling through JNK phosphorylation. LPC-induced JNK activation was not affected by transfection of iPLA₂β or iPLA₂γ siRNA, as expected (Fig. 5C). Exogenous LPC also decreased insulin-induced 2-deoxyglucose uptake by L6 myotubes (*P* < 0.05) (Fig. 5D), suggesting that LPC induces insulin resistance through JNK activation. We also tested the effect of blockade of G-protein coupled receptor (GPCR) by pertussis toxin (PTX) on PA-induced insulin resistance because PTX has been reported to inhibit most LPC signaling through GPCR/Gα_i (30, 31). PTX reversed the decreased insulin-induced IRS-1 Tyr612 and Akt phosphorylation by LPC or PA (Fig. 5E, F) and ameliorated JNK activation by PA (Fig. 5G), suggesting that LPC

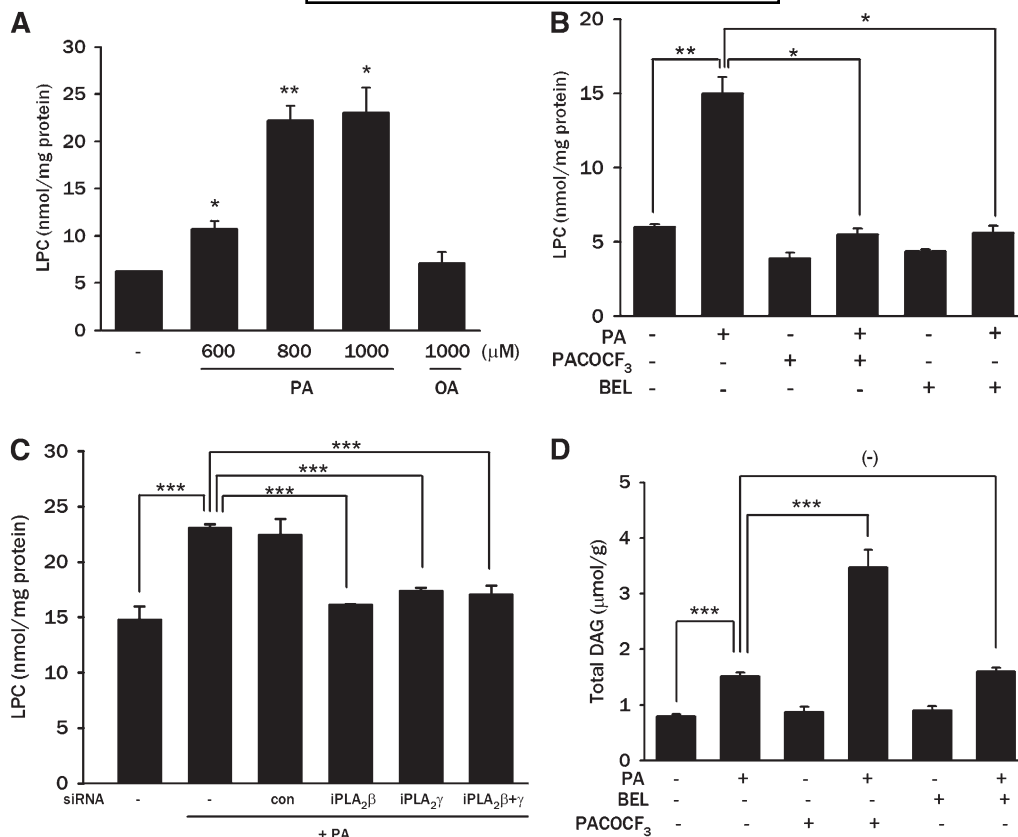


Fig. 4. Intracellular contents of LPC and DAG after PA treatment. **A:** After treatment of L6 myotubes with the indicated concentrations of PA or OA for 12 h, myotubes were lysed, and intracellular LPC content was measured by an enzymatic assay as described in Materials and Methods. **B:** After pretreatment with 100 μM PACOCF₃ or 10 μM BEL for 1 h, L6 myotubes were treated with 800 μM PA for 12 h, and intracellular LPC content was measured as in A. **C:** After transfection of L6 myotubes with iPLA₂β siRNA, iPLA₂γ siRNA, or control siRNA (Con), myotubes were treated with 800 μM PA for 12 h, and intracellular LPC content was measured as in A. **D:** L6 myotubes were treated with 600 μM PA for 12 h after pretreatment with 100 μM PACOCF₃ or 10 μM BEL for 1 h. Content of total intracellular DAG was measured as described in Materials and Methods. The values (means ± SE) are representative of three or four independent experiments performed in triplicate showing similar tendencies. **P* < 0.05; ***P* < 0.01; ****P* < 0.005.

induces insulin resistance through GPCR/Gα_i. Because LPC can be incorporated into DAG or other lipid metabolites through autotoxin or other pathways (32), we measured the content of lipids that can affect insulin signaling. DAG, ceramide, and TG contents were not significantly changed after LPC treatment (*P* > 0.1 for all comparisons) (supplementary Fig. IV), indicating that the effect of exogenous LPC on insulin signaling is not related to its conversion to other lipid intermediates potentially involved in the modulation of insulin signaling.

In vivo effect of LPC modulation on diabetes

Because these in vitro results suggested an important role for LPC generated from PA in insulin resistance, we determined whether BEL, an inhibitor of endogenous production of LPC from FFA in vitro, could attenuate insulin resistance and diabetes in vivo. When 200 μg/kg of BEL was administered to *db/db* mice, a significant decrease in the nonfasting blood glucose level was noted after one week of treatment compared with control *db/db* mice treated with vehicle alone (*P* < 0.005–0.01). Treated mice remained normoglycemic throughout the four-week treatment period, while all of the

control *db/db* mice became diabetic during the same observation period (Fig. 6A). The body weights were not significantly different between the two groups (*P* > 0.05), suggesting that BEL lowers blood glucose without affecting appetite and does not have significant systemic toxicity (Fig. 6B). Indeed, food intake was not significantly different between the *db/db* mice treated with BEL and control *db/db* mice (supplementary Fig. V). IPGTT showed that BEL treatment for four weeks dramatically improved glucose tolerance in *db/db* mice (*P* < 0.005–0.05) (Fig. 6C). The HOMA-IR index was significantly decreased by BEL treatment for four weeks in *db/db* mice (*P* < 0.005) (Fig. 6D), supporting the finding that BEL treatment improves insulin resistance. The ITT also showed that K_{ITT}, another index of insulin resistance (33), was significantly improved by the administration of BEL to *db/db* mice (−0.37 ± 0.15%/min in vehicle-treated *db/db* mice versus 2.12 ± 0.62%/min in BEL-treated *db/db* mice; *n* = 8 each; *P* < 0.005). In contrast, BEL administration did not affect the blood glucose level, body weight, or HOMA-IR in C57BL/6 mice (*P* > 0.05 for all comparisons) (Fig. 6A–D).

To elucidate the mechanism underlying the improvement in the glycemic profile by BEL, we examined whether

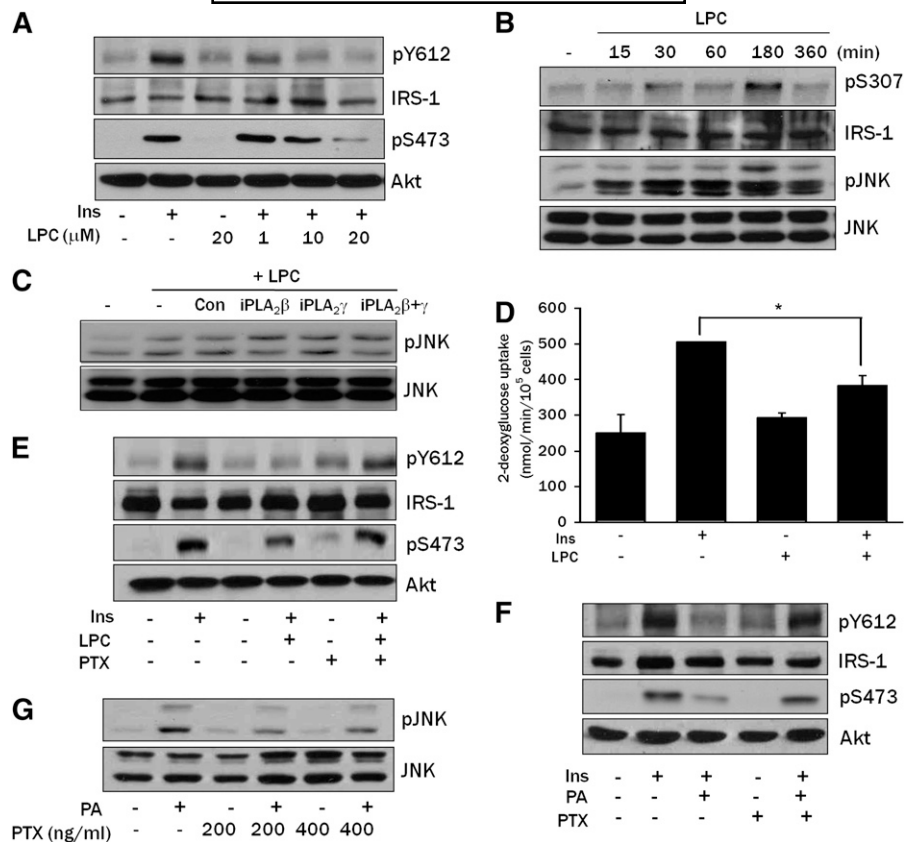


Fig. 5. Effect of exogenous LPC on insulin signaling. **A:** L6 myotubes were treated with the indicated concentrations of LPC for 3 h, then stimulated with 100 nM insulin for 15 min. Cell lysates were subjected to Western blotting to determine phosphorylation of IRS-1 Tyr612 and Akt Ser473 as in Fig. 1A. **B:** L6 myotubes were treated with 20 μ M LPC for the indicated time periods. Cell lysates were subjected to Western blotting to determine phosphorylation of JNK and IRS-1 Ser307 as in Fig. 1C. **C:** After transfection of L6 myotubes with iPLA₂ β siRNA, iPLA₂ γ siRNA, or control siRNA (Con), myotubes were treated with 20 μ M LPC for 3 h. Cell lysates were prepared for Western blotting as in B. **D:** After treatment with 20 μ M LPC for 3 h, L6 myotubes were treated with 100 nM insulin for 30 min. Uptake of 2-deoxyglucose was measured as in Fig. 1B. **E** and **F:** L6 myotubes were pretreated with 100 ng/ml PTX for 1 h, then incubated with 20 μ M LPC for 3 h (E) or with 800 μ M PA for 14 h (F). After treatment with 100 nM insulin for 15 min, cell lysates were subjected to Western blotting to determine phosphorylation of IRS-1 Tyr612 or Akt Ser473 using specific antibodies. **G:** L6 myotubes were pretreated with PTX for 1 h, then incubated with 800 μ M PA for 14 h. Cell lysates were subjected to Western blotting using an antibody specific for phospho-JNK. All results shown are representative of two to four independent experiments. * $P < 0.05$.

BEL could affect LPC content in the insulin target tissues in vivo. Consistent with our hypothesis that LPC is an important mediator of insulin resistance, the LPC content was increased in the liver and muscle of *db/db* mice compared with C57BL/6 mice ($P < 0.005$ and $P < 0.01$, respectively) (Fig. 7A). Furthermore, BEL treatment for four weeks significantly lowered the increased LPC content in both tissues ($P < 0.05$ for both comparisons) (Fig. 7A), suggesting that BEL improves blood glucose profiles by normalizing LPC content. Next, we studied whether BEL treatment in vivo could affect JNK activation since LPC could be an inducer of JNK activation after FFA treatment (26). JNK was activated in the liver and muscle of the *db/db* mice as previously reported, and the increased JNK activation in *db/db* mice was significantly ameliorated by BEL treatment for four weeks (Fig. 7B), consistent with our hypothesis that LPC generated from PA induces insulin resistance through JNK activation. BEL treatment for four

weeks also attenuated the increased IRS-1 Ser307 phosphorylation in the liver and muscle of *db/db* mice (Fig. 7B). Probably because of the decreased JNK activation and IRS-1 Ser307 phosphorylation, BEL treatment for four weeks restored the diminished IRS-1 Tyr612 and Akt Thr308 phosphorylation after insulin injection in the liver and muscle of *db/db* mice (Fig. 7C).

Concomitant with the ameliorated insulin resistance, the serum insulin level was significantly reduced ($P < 0.05$) (Fig. 7D) and the pancreatic β -cell mass was significantly increased ($P < 0.01$) after BEL administration to *db/db* mice for four weeks (Fig. 7E).

DISCUSSION

We observed that PA induced insulin resistance in L6 myotubes through JNK activation between 6 and 12 h unlike OA, which is consistent with previous studies using

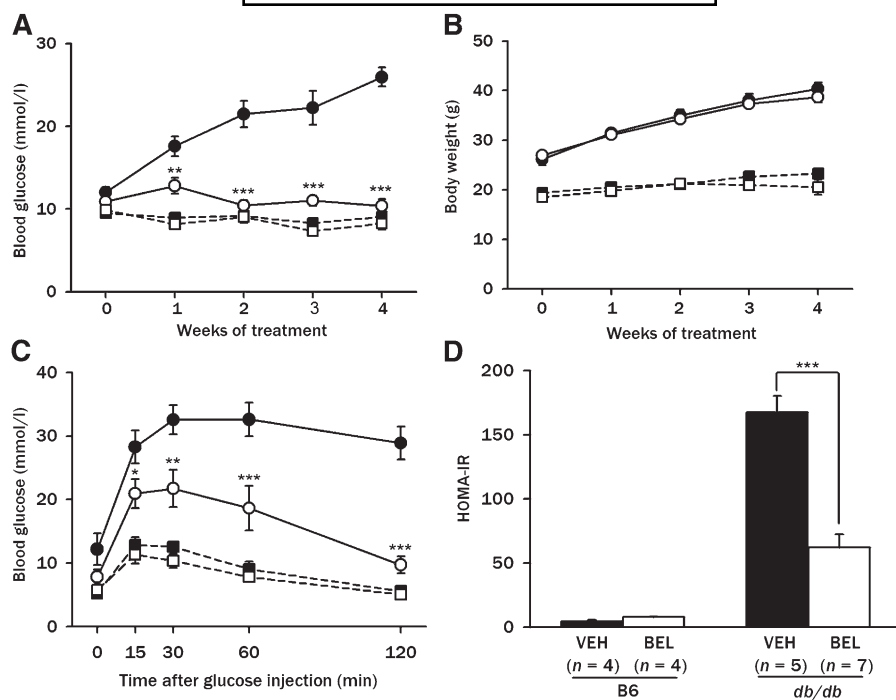


Fig. 6. Effect of BEL on diabetes of *db/db* mice. A: BEL (200 μ g/kg) or vehicle (VEH) was administered intraperitoneally to 5-week-old *db/db* and C57BL/6 control mice three times a week for four weeks. Nonfasting blood glucose levels were determined using a glucometer. B: Body weight was monitored throughout the treatment period. C: An IPGTT was conducted by injecting 1 mg/kg of glucose intraperitoneally to *db/db* or C57BL/6 control mice treated with 200 μ g/kg BEL or vehicle for four weeks, and blood glucose levels were measured at the indicated time points. D: HOMA-IR index was calculated as described in Materials and Methods. Results pooled from three independent experiments are presented. * $P < 0.05$; ** $P < 0.01$; *** $P < 0.005$. ●, *db/db*-VEH (A–C, $n = 12$); ○, *db/db*-BEL (A–C, $n = 12$); ■, C57BL/6-VEH (A–C, $n = 8$); □, C57BL/6-BEL (A–C, $n = 8$).

hepatocytes (20, 34). OA induced a weak activation of JNK at an early time point, which could be through a mechanism, such as FFA receptor binding (35), distinct from PA-induced JNK activation. In fact, PA also induced a weak JNK activation at the same early time point (Fig. 1C), which could be due to binding of PA and OA to the same FFA receptors and might be mechanistically different from JNK activation by PA but not by OA at later time points due to the conversion of PA to other lipid metabolites such as LPC.

In our search for effector molecule(s) in insulin resistance by FFA, we found evidence suggesting that LPC generated from saturated FFA via phosphatidic acid, DAG, and PC, is an effector for JNK activation, IRS-1 Ser307 phosphorylation, and insulin resistance. TG, DAG, or ceramide could be candidates for possible effector molecules in FFA-induced insulin resistance. Evidence supporting the role of TG in obesity-induced insulin resistance is mostly from the association between intracellular TG content and insulin resistance (36–38). However, biochemical data substantiating the etiological role of TG in obesity- or FFA-induced insulin resistance are lacking. Furthermore, unsaturated FFA led to increased intracellular TG content but did not significantly activate JNK, while saturated FFA did not significantly increase intracellular TG content but was a strong inducer of JNK activation and insulin resistance (9, 20, 39). These results suggest that TG is not a direct effector molecule causing JNK activation and insu-

lin resistance. DAG could be another candidate for the effector in FFA-induced insulin resistance because FFA could be converted to DAG intracellularly through phosphatidic acid (7), and DAG is a well-known activator of PKC that could mediate insulin resistance (40). However, we observed that iPLA₂ inhibitors, such as BEL or PACOCF₃, significantly inhibited JNK activation and insulin resistance by PA, while increasing intracellular DAG content. Because DAG could be converted to PC and then to LPC, a well-known activator of JNK, by PLA₂ (26, 41), our results, which showed a substantial inhibition of FFA-induced insulin resistance by BEL or PACOCF₃, suggest the involvement of iPLA₂ and LPC rather than DAG upstream of PLA₂ in FFA-induced JNK activation and insulin resistance. While BEL has been reported to inhibit PAP in addition to iPLA₂ (28), our finding that PACOCF₃, another iPLA₂-specific inhibitor structurally unrelated to BEL (28), also strongly inhibited insulin resistance by PA, suggests that iPLA₂ and LPC play a role in FFA-induced JNK activation and insulin resistance. The increase of DAG by BEL was less than that by PACOCF₃, likely because of concomitant inhibition of PAP by BEL (28). The biochemical mechanism underlying the preferential increase of LPC by PA but not by OA is not clearly understood. OA might be more prone to be directed to other pathways, such as TG synthesis or β -oxidation, as was shown in the current study (supplementary Fig. III) and previous reports (9, 42).

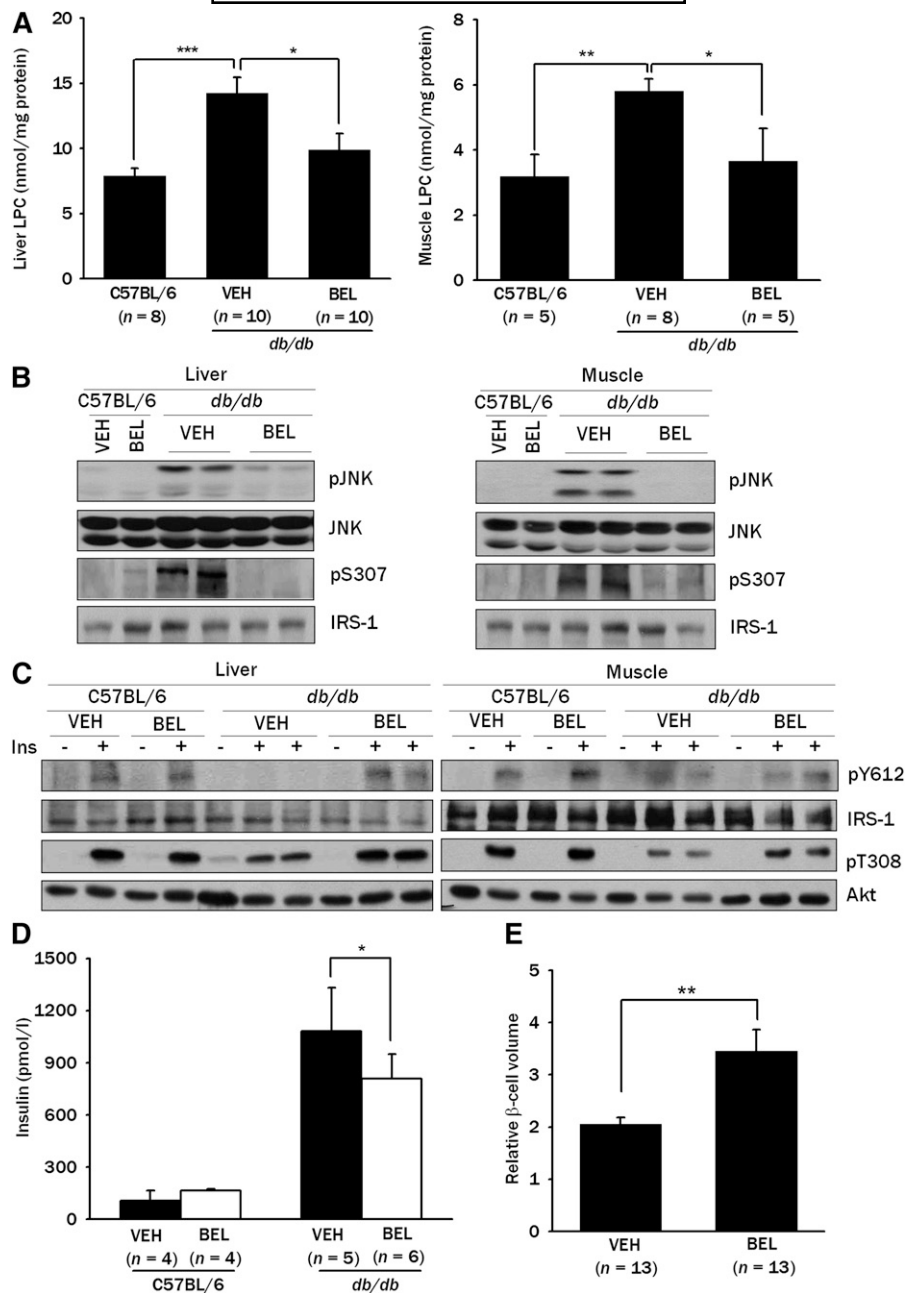


Fig. 7. LPC content in vivo. **A:** LPC content in the liver and muscle tissues from *db/db* or C57BL/6 control mice treated with 200 μ g/kg of BEL or vehicle (VEH) for four weeks was measured as in Fig. 4A. **B:** Tissue lysates of the liver and muscle from *db/db* and C57BL/6 control mice treated with 200 μ g/kg of BEL or vehicle for four weeks were subjected to Western blotting to determine phosphorylation of JNK and IRS-1 Ser307. **C:** An amount of 5 U/kg of regular insulin was injected into the tail vein of the *db/db* or control C57BL/6 mice treated with 200 μ g/kg of BEL or vehicle for four weeks. After 5 min, tissue lysates of the liver and muscle from *db/db* and C57BL/6 control mice were prepared, and the tissue lysates were subjected to Western blotting to assess phosphorylation of IRS-1 Tyr612 and Akt Thr308. **D:** Serum was obtained from fasted *db/db* mice or control C57BL/6 mice treated with 200 μ g/kg of BEL or vehicle for four weeks, and insulin levels were measured by RIA. **E:** After insulin immunohistochemistry of pancreatic sections from *db/db* mice treated with 200 μ g/kg of BEL or vehicle for four weeks was carried out, point counting morphometry was conducted to measure the relative β -cell volume. Representative values (means \pm SE) from three independent experiments are presented in A. Western blots are representative of three independent experiments. * $P < 0.05$; ** $P < 0.01$; *** $P < 0.005$.


Ceramide is another strong candidate for the effector molecule in obesity- or FFA-induced insulin resistance (4, 5, 43). However SPT, the enzyme catalyzing the initial step in de novo synthesis of ceramide from PA, has a specificity

toward PA, and other saturated fatty acids, such as stearic acid or myristic acid, are poor substrates for SPT (44). Therefore, de novo synthesis of ceramide may play a role in insulin resistance when PA is involved but not when

other saturated FFA, such as stearic acid, is involved, while stearic acid or myristic acid well induces JNK activation and insulin resistance (20, 45). Previous studies have also reported that the production of TNF α and IL-6, which are implicated in obesity- or FFA-induced insulin resistance, was not affected by ceramide synthesis inhibitors (46, 47), suggesting that de novo synthesis of ceramide may not play an important role in insulin resistance induced by obesity or FFA.

Our data suggesting the role of endogenous LPC in FFA-induced insulin resistance is supported by the significantly elevated intracellular content of LPC after PA treatment of L6 myotubes that did not occur in the presence of iPLA₂ inhibitors, such as PACOCF₃ or BEL. The mechanism of the increase in LPC content after PA treatment might be related to the induction of genes involved in the conversion of PA to LPC. However, the main cause of the increase of LPC after PA treatment could be the increase in the amount of substrate. In fact, we observed no significant change of iPLA₂ β or iPLA₂ γ expression after PA treatment of L6 myotubes (W. Quan et al., unpublished data). Induction of insulin resistance by exogenous LPC, which is consistent with the findings of a previous study (27), also substantiates the role of endogenous LPC in FFA-induced insulin resistance. Because potential receptors for LPC, such as GPCR, may recognize extracellular ligands, LPC might be released to the extracellular space and bind to GPCR (48). Or LPC might enter the receptor-binding site in a lateral fashion between transmembrane regions of the receptor without leaving the membrane (49). However, it is not clear which among several types of PLA₂ is responsible for the production of endogenous LPC after FFA treatment of L6 myotubes. While we observed a significant decrease in FFA-induced insulin resistance by iPLA₂ β or iPLA₂ γ siRNA, our data alone cannot eliminate the potential role of other types of PLA₂. Although our previous results using a lipopoptosis model (9) and the current data showing improvement of insulin resistance and diabetes by selective iPLA₂ inhibitors demonstrate important roles of iPLA₂ in lipid injury, further work will be necessary to elucidate the roles for various PLA₂ types in FFA-induced insulin resistance.

Our in vitro data showing the role of endogenous LPC generated from FFA by iPLA₂ in FFA-induced JNK activation and insulin resistance suggest the possibility that modulation of endogenous LPC content could be a strategy to treat obesity-induced diabetes, corroborated by our in vivo data showing that administration of BEL ameliorated JNK activation, insulin resistance, and diabetes in *db/db* mice by decreasing LPC content in the liver and muscle. A previous study showed that *iPLA₂ β* -null mice have impaired insulin secretion but improved insulin sensitivity on a high-fat diet (50), which might be due to decreased LPC content in insulin target tissues. The relatively mild effect of targeted disruption of *iPLA₂ β* compared with that of BEL treatment could be due to compensatory changes in *iPLA₂ β* -null mice or potential effects of BEL on iPLA₂ subtypes other than iPLA₂ β . In agreement with this idea, recent studies have shown that targeted disruption of *iPLA₂ γ* leads to prevention of high-fat, diet-induced insulin resistance (51, 52).

While we focused on the role of LPC as an effector of insulin resistance in the current study, we previously reported that LPC could be an effector in lipopoptosis (9). Reports by other investigators have shown that PLA₂ is involved in several cellular injury models and that iPLA₂ inhibitors could decrease tissue damage by various stressors (53, 54). The increase in β -cell mass after BEL administration to *db/db* mice observed in our study could be due to decreased β -cell stress following reduced insulin resistance or direct protective effect of iPLA₂ inhibitors against lipid injury or lipopoptosis of β -cells. Hence, LPC could be involved in the pathogenesis of type 2 diabetes by inducing insulin resistance in insulin target tissue and by imposing islet cell injury. Altogether, our results suggest that LPC, in addition to the previously reported metabolites, such as ceramide or DAG, could be an effector molecule in FFA-induced insulin resistance via JNK activation, and that iPLA₂ inhibitors could be employed as potential therapeutic agents against diabetes associated with obesity or lipid injury. 

REFERENCES

1. Reaven, G. M., C. Hollenbeck, C. Y. Jeng, M. S. Wu, and Y. D. Chen. 1988. Measurement of plasma glucose, free fatty acid, lactate, and insulin for 24 h in patients with NIDDM. *Diabetes*. **37**: 1020–1024.
2. Roden, M., T. B. Price, G. Perseghin, K. F. Petersen, D. L. Rothman, G. W. Cline, and G. I. Shulman. 1996. Mechanism of free fatty acid-induced insulin resistance in humans. *J. Clin. Invest.* **97**: 2859–2865.
3. Zhou, Y. P., and V. E. Grill. 1994. Long-term exposure of rat pancreatic islets to fatty acids inhibits glucose-induced insulin secretion and biosynthesis through a glucose fatty acid cycle. *J. Clin. Invest.* **93**: 870–876.
4. Shimabukuro, M., M. Y. Wang, Y. T. Zhou, C. B. Newgard, and R. H. Unger. 1998. Protection against lipopoptosis of beta cells through leptin-dependent maintenance of Bcl-2 expression. *Proc. Natl. Acad. Sci. USA*. **95**: 9558–9561.
5. Holland, W. L., J. T. Brozinick, L. P. Wang, E. D. Hawkins, K. M. Sargent, Y. Liu, K. Narra, K. L. Hoehn, T. A. Knotts, A. Siesky, et al. 2007. Inhibition of ceramide synthesis ameliorates glucocorticoid-, saturated-fat-, and obesity-induced insulin resistance. *Cell Metab.* **5**: 167–179.
6. Koves, T. R., J. R. Ussher, R. C. Noland, D. Slentz, M. Mosedale, O. Ilkayeva, J. Bain, R. Stevens, J. R. Dyck, C. B. Newgard, et al. 2008. Mitochondrial overload and incomplete fatty acid oxidation contribute to skeletal muscle insulin resistance. *Cell Metab.* **7**: 45–56.
7. Montell, E., M. Turini, M. Marotta, M. Roberts, V. Noe, C. J. Ciudad, K. Mace, and A. M. Gomez-Foix. 2001. DAG accumulation from saturated fatty acids desensitizes insulin stimulation of glucose uptake in muscle cells. *Am. J. Physiol.* **280**: E229–E237.
8. Perseghin, G., P. Scifo, F. De Cobelli, E. Pagliato, A. Battezzati, C. Arcelloni, A. Vanzulli, G. Testolin, G. Pozza, A. del Maschio, et al. 1999. Intramyocellular triglyceride content is a determinant of in vivo insulin resistance in humans. *Diabetes*. **48**: 1600–1606.
9. Han, M. S., S. Y. Park, K. Shinzawa, S. Kim, K. W. Chung, J. H. Lee, C. H. Kwon, K. W. Lee, J.-H. Lee, C. K. Park, et al. 2008. Lysophosphatidylcholine as a death effector in lipopoptosis of hepatocytes. *J. Lipid Res.* **49**: 84–97.
10. Niu, W., C. Huang, Z. Nawaz, M. Levy, R. Somwar, D. Li, P. J. Bilan, and A. Klip. 2003. Maturation of the regulation of GLUT4 activity by p38 MAPK during L6 cell myogenesis. *J. Biol. Chem.* **278**: 17953–17962.
11. Niu, M., J. C. Hannaert, A. Hoorens, D. L. Elizirik, and D. G. Pipeleers. 2001. Inverse relationship between cytotoxicity of free fatty acids in pancreatic islet cells and cellular triglyceride accumulation. *Diabetes*. **50**: 1771–1777.
12. Pacheco, Y. M., M. C. Pérez-Camino, A. Cert, E. Montero, and V. Ruiz-Gutiérrez. 1998. Determination of the molecular species composition of diacylglycerols in human adipose tissue by solid-phase

- extraction and gas chromatography on a polar phase. *J. Chromatogr. B Biomed. Sci. Appl.* **714**: 127–132.
13. Yu, C., Y. Chen, G. W. Cline, D. Zhang, H. Zong, Y. Wang, R. Bergeron, J. K. Kim, S. W. Cushman, G. J. Cooney, et al. 2002. Mechanism by which fatty acids inhibit insulin activation of insulin receptor substrate-1 (IRS-1)-associated phosphatidylinositol 3-kinase activity in muscle. *J. Biol. Chem.* **277**: 50230–50236.
 14. Yoo, H. H., J. Son, and D-H. Kim. 2006. Liquid chromatography-tandem mass spectrometric determination of ceramides and related lipid species in cellular extracts. *J. Chromatogr. B Analyt. Technol. Biomed. Life Sci.* **843**: 327–333.
 15. Han, M. S., K. W. Chung, H. G. Cheon, S. D. Rhee, C. H. Yoon, M. K. Lee, K. W. Kim, and M. S. Lee. 2009. Imatinib mesylate reduces endoplasmic reticulum stress and induces remission of diabetes in db/db mice. *Diabetes.* **58**: 329–336.
 16. Kozma, L., K. Baltensperger, J. Klarlund, A. Porras, E. Santos, and M. P. Czech. 1993. The ras signaling pathway mimics insulin action on glucose transporter translocation. *Proc. Natl. Acad. Sci. USA.* **90**: 4460–4464.
 17. Kaku, K., F. T. Fiedorek, M. Province, and A. Permutt. 1988. Genetic analysis of glucose tolerance in inbred mouse strains-evidence for polygenic control. *Diabetes.* **37**: 707–713.
 18. Cai, D., M. Yuan, D. F. Frantz, P. A. Melendez, L. Hansen, J. Lee, and S. E. Shoelson. 2005. Local and systemic insulin resistance resulting from hepatic activation of IKK-beta and NF-kappaB. *Nat. Med.* **11**: 183–190.
 19. Hirosumi, J., G. Tuncman, L. Chang, C. Z. Gorgun, K. T. Uysal, K. Maeda, M. Karin, and G. S. Hotamisligil. 2002. A central role for JNK in obesity and insulin resistance. *Nature.* **420**: 333–336.
 20. Solinas, G., W. Naugler, F. Galimi, M-S. Lee, and M. Karin. 2006. Saturated fatty acids inhibit induction of insulin gene transcription by JNK-mediated phosphorylation of insulin-receptor substrates. *Proc. Natl. Acad. Sci. USA.* **103**: 16454–16459.
 21. Lee, Y. H., J. Giraud, R. J. Davis, and M. F. White. 2003. c-Jun N-terminal kinase (JNK) mediates feedback inhibition of the insulin signaling cascade. *J. Biol. Chem.* **278**: 2896–2902.
 22. Merrill, A. H., Jr., G. van Echten, E. Wang, and K. Sandhoff. 1993. Fumonisin B1 inhibits sphingosin (sphinganine) N-acyltransferase and de novo sphingolipid biosynthesis in cultured neurons in situ. *J. Biol. Chem.* **268**: 27299–27306.
 23. Tonnetti, L., M. C. Veri, E. Bonvini, and L. D'Adamio. 1999. A role for neutral sphingomyelinase-mediated ceramide production in T cell receptor-induced apoptosis and mitogen-activated protein kinase-mediated signal transduction. *J. Exp. Med.* **189**: 1581–1589.
 24. Chalfant, C. E., B. Ogretmen, S. Galadari, B-J. Kroesen, B. J. Pettus, and Y. A. Hannun. 2001. FAS activation induces dephosphorylation of SR proteins. *J. Biol. Chem.* **276**: 44848–44855.
 25. Ogretmen, B., B. J. Pettus, M. J. Rossi, R. Wood, J. Usta, Z. Szule, A. Bielawska, L. M. Obeid, and Y. A. Hannun. 2002. Biochemical mechanisms of the generation of endogenous long chain ceramide in response to exogenous short chain ceramide in the A549 human lung adenocarcinoma cell line. *J. Biol. Chem.* **277**: 12960–12969.
 26. Fang, X., S. Gibson, M. Flowers, T. Furui, R. C. Bast, Jr., and G. B. Mills. 1997. Lysophosphatidylcholine stimulates activator protein 1 and the c-Jun N-terminal kinase activity. *J. Biol. Chem.* **272**: 13683–13689.
 27. Motley, E. D., S. M. Kabir, C. D. Gardner, K. Eguchi, G. D. Frank, T. Kuroki, M. Ohba, T. Yamakawa, and S. Eguchi. 2002. Lysophosphatidylcholine inhibits insulin-induced Akt activation through protein kinase C-alpha in vascular smooth muscle cells. *Hypertension.* **39**: 508–512.
 28. Balsinde, J., and E. A. Dennis. 1996. Bromoenol lactone inhibits magnesium-dependent phosphatidate phosphohydrolase and blocks triacylglycerol biosynthesis in mouse P388D1 macrophages. *J. Biol. Chem.* **271**: 31937–31941.
 29. Ostrander, D. B., G. C. Sparagna, A. A. Amoscato, J. B. McMillin, and W. Dowhan. 2001. Decreased cardiolipin synthesis corresponds with cytochrome c release in palmitate-induced cardiomyocyte apoptosis. *J. Biol. Chem.* **276**: 38061–38067.
 30. Kabarowski, J. H. S., K. Zhu, L. Q. Le, O. N. Witte, and Y. Xu. 2001. Lysophosphatidylcholine as a ligand for the immunoregulatory receptor G2A. *Science.* **293**: 702–705.
 31. Zhu, K., L. B. Baudhuin, G. Hong, F. S. Williams, K. L. Cristina, J. H. S. Kabarowski, O. N. Witte, and Y. Xu. 2001. Sphingosylphosphorylcholine and lysophosphatidylcholine are ligands for the G protein-coupled receptor GPR4. *J. Biol. Chem.* **276**: 41325–41335.
 32. Hama, K., J. Aoki, M. Fukaya, Y. Kishi, T. Sakai, R. Suzuki, H. Ohta, T. Yamori, M. Watanabe, J. Chun, et al. 2004. Lysophosphatidic acid and autotaxin stimulate cell motility of neoplastic and non-neoplastic cells through LPA1. *J. Biol. Chem.* **279**: 17634–17639.
 33. Phillips, D. I., P. M. Clark, C. N. Hales, and C. Osmond. 1993. Understanding oral glucose tolerance: comparison of glucose or insulin measurements during the oral glucose tolerance test with specific measurements of insulin resistance and insulin secretion. *Diabet. Med.* **11**: 286–292.
 34. Nakamura, S., T. Takamura, N. Matsuzawa-Nagata, H. Takayama, H. Misu, H. Noda, S. Nabemoto, S. Kurita, T. Ota, H. Ando, et al. 2009. Palmitate induces insulin resistance in H4IIEC3 hepatocytes through reactive oxygen species produced by mitochondria. *J. Biol. Chem.* **284**: 14809–14818.
 35. Itoh, Y., Y. Kawamata, M. Harada, M. Kobayashi, R. Fujii, S. Fukusumi, K. Ogi, M. Hosoya, Y. Tanaka, H. Uejima, et al. 2003. Free fatty acids regulate insulin secretion from pancreatic beta cells through GPR40. *Nature.* **422**: 173–176.
 36. Avignon, A., K. Yamada, X. Zhou, B. Spencer, O. Cardona, S. Saba-Siddique, L. Galloway, M. L. Standaert, and R. V. Farese. 1996. Chronic activation of protein kinase C in soleus muscles and other tissues of insulin-resistant type II diabetic Goto-Kakizaki (GK), obese/aged, and obese/Zucker rats. A mechanism for inhibiting glycogen synthesis. *Diabetes.* **45**: 1396–1404.
 37. Krssak, M., P. K. Falk, A. Dresner, L. DiPietro, S. M. Vogel, D. L. Rothman, M. Roden, and G. I. Shulman. 1999. Intramyocellular lipid concentrations are correlated with insulin sensitivity in humans: a ¹H NMR spectroscopy study. *Diabetologia.* **42**: 113–116.
 38. Pan, D. A., S. Lillioja, A. D. Krisquetos, M. R. Milner, L. A. Baur, C. Bogardus, A. B. Jenkins, and L. H. Storlien. 1997. Skeletal muscle triglyceride levels are inversely related to insulin action. *Diabetes.* **46**: 983–988.
 39. Listenberger, L. L., X. Han, S. E. Lewis, S. Cases, R. V. Farese, D. S. Ory, and J. E. Schaffer. 2003. Triglyceride accumulation protects against fatty acid-induced lipotoxicity. *Proc. Natl. Acad. Sci. USA.* **100**: 3077–3082.
 40. Eitel, K., H. Staiger, J. Rieger, H. Mischak, H. Brandhorst, M. D. Brendel, R. G. Bretzel, H. U. Haring, and M. Kellerer. 2003. Protein kinase C delta activation and translocation to the nucleus are required for fatty acid-induced apoptosis of insulin-secreting cells. *Diabetes.* **52**: 991–997.
 41. Takahashi, M., H. Okazaki, Y. Ogata, K. Takeuchi, U. Ikeda, and K. Shimada. 2002. Lysophosphatidylcholine induces apoptosis in human endothelial cells through a p38-mitogen-activated protein kinase-dependent mechanism. *Atherosclerosis.* **161**: 387–394.
 42. Coll, T., E. Eyre, R. Rodriguez-Calvo, X. Palomer, R. M. Sanchez, M. Merlos, J. C. Laguna, and M. Vazquez-Carrera. 2008. Oleate reverses palmitate-induced insulin resistance and inflammation in skeletal muscle cells. *J. Biol. Chem.* **283**: 11107–11116.
 43. Schmitz-Peiffer, C., D. L. Craig, and T. J. Biden. 1999. Ceramide generation is sufficient to account for the inhibition of the insulin-stimulated PKB pathway in C2C12 skeletal muscle cells pretreated with palmitate. *J. Biol. Chem.* **274**: 24202–24210.
 44. Hanada, K. 2003. Serine palmitoyltransferase, a key enzyme of sphingolipid metabolism. *Biochim. Biophys. Acta.* **1632**: 16–30.
 45. Song, M. J., K. H. Kim, J. M. Yoon, and J. B. Kim. 2006. Activation of Toll-like receptor 4 is associated with insulin resistance in adipocytes. *Biochem. Biophys. Res. Commun.* **346**: 739–745.
 46. Jove, M., A. Planavila, J. C. Laguna, and M. Vazquez-Carrera. 2005. Palmitate-induced interleukin 6 production is mediated by protein kinase C and nuclear-factor kappaB activation and leads to glucose transporter 4 down-regulation in skeletal muscle cells. *Endocrinology.* **146**: 3087–3095.
 47. Jove, M., A. Planavila, R. M. Sanchez, M. Merlos, J. C. Laguna, and M. Vazquez-Carrera. 2006. Palmitate induces tumor necrosis factor-alpha expression in C2C12 skeletal muscle cells by a mechanism involving protein kinase C and nuclear factor-kappaB activation. *Endocrinology.* **147**: 552–561.
 48. van den Besselaar, A. M., B. de Kruijff, H. van den Bosch, and L. L. van Deenen. 1979. Transverse distribution and movement of lysophosphatidylcholine in sarcoplasmic reticulum membranes as determined by ¹³C NMR and lysophospholipase. *Biochim. Biophys. Acta.* **555**: 193–199.
 49. Xie, Y., T. C. Gibbs, and K. E. Meier. 2002. Lysophosphatidic acid as an autocrine and paracrine mediator. *Biochim. Biophys. Acta.* **1582**: 270–281.
 50. Bao, S., H. Song, M. Wohltmann, S. Ramanadham, W. Jin, A. Bohrer, and J. Turk. 2006. Insulin secretory responses and phospholipid composition of pancreatic islets from mice that do not

express group VIA phospholipase A2 and effects of metabolic stress on glucose homeostasis. *J. Biol. Chem.* **281**: 20958–20973.

51. Mancuso, D. J., H. F. Sims, K. Yang, M. A. Kiebish, X. Su, C. M. Jenkins, S. Guan, S. H. Moon, T. Pietka, F. Nassir, et al. 2010. Genetic ablation of calcium-independent phospholipase A2gamma prevents obesity and insulin resistance during high fat feeding by mitochondrial uncoupling and increased adipocyte fatty acid oxidation. *J. Biol. Chem.* **285**: 36495–36510.
52. Song, H., M. Wohltmann, S. Bao, J. H. Ladenson, C. F. Semenkovich, and J. Turk. 2010. Mice deficient in group VIB phospholipase A2 (iPLA2gamma) exhibit relative resistance to obesity and metabolic abnormalities induced by a Western diet. *Am. J. Physiol. Endocrinol. Metab.* **298**: E1097–E1114.
53. Shinzawa, K., and Y. Tsujimoto. 2003. PLA2 activity is required for nuclear shrinkage in caspase-independent cell death. *J. Cell Biol.* **163**: 1219–1230.
54. Cauwels, A., B. Janssen, A. Waeytens, C. Cuvelier, and P. Brouckaert. 2003. Caspase inhibition causes hyperacute tumor necrosis factor-induced shock via oxidative stress and phospholipase A2. *Nat. Immunol.* **4**: 387–393.